J Petrol Explor Prod Technol (2018) 8:363–374
https://doi.org/10.1007/s13202-017-0400-9

ORIGINAL PAPER - EXPLORATION GEOLOGY

Depositional environments and petrofacies of X–XII sand groups of K_2qn^3 Formation, Daqingzijing area, Songliao Basin, China

Congjun Feng[1,2,3] · Weicheng Shi[4] · Yong Hu[5] · Xinghui Zhao[2,3]

Received: 17 July 2016 / Accepted: 13 October 2017 / Published online: 28 October 2017

Abstract Integration of the geological context, core analysis, and petrographic investigation, together with data from wireline logs, resulted in the recognition of petrofacies types and the representation of facies models characterizing the X–XII sand groups of the K_2qn^3 Formation in the Daqingzijing area of the Songliao Basin, China. The results show that the lithology of the reservoir's X–XII sand groups includes shale calcium-bearing siltstone and sandstone, calcareous siltstone and silty sandstone. The petrofacies consist mainly of quartz, feldspar and rock fragments cemented by clay, and some samples include calcite. The studied interval was deposited onto a delta front. Four types of petrofacies were recognized: subaqueous distributary channel, mouth bar, distal bar and subaqueous interdistributary bay. According to background investigation, the study area's X–XII sand groups have experienced a large-scale decline in lake level. There are many subaqueous distributary channels in layers 36–40, while other layers were mainly deposited in a subaqueous interdistributary bay.

Keywords Sedimentary petrofacies · Subaqueous distributary channel · Mouth bar · Songliao Basin

Introduction

The study of sedimentary petrofacies is at the core and foundation of reservoir geology. Macroscopically, it controls the geometry and spatial distribution of a reservoir sand body (Zhang et al. 2010; Li et al. 2013), and microscopically, it controls the different physical properties and heterogeneity of a reservoir (Liu et al. 2014; Zeng et al. 2013). Therefore, sedimentary petrofacies have always been the focus of attention and a hot issue in the research field of reservoir sedimentology (Zhang et al. 2009; Cao et al. 2010). Sedimentary petrofacies of different geneses reflect the ancient environment, hydrodynamic conditions, material sources and so on of the original sedimentary deposits (Zhang et al. 2007; Zhu et al. 2012). Facies sequences of different types reflect certain characteristics, such as the supply rate, evolution of the sedimentary system, fluctuations of lakes and tectonic evolution, during the process of sediment deposition (Zhang et al. 2011; Er et al. 2013). Different types of sedimentary petrofacies can control the physical properties and heterogeneity of a reservoir. The better the sediment particle sorting is, and the lower the shale content is, the more the intergranular porosity can be maintained, to provide a channel for the migration of acid fluid in a later period. Therefore, it is easy to form a reservoir with good physical properties (Zou et al. 2004; Zhang et al. 2006; Feng et al. 2013). In the process of oilfield water injection development,

✉ Congjun Feng
fengcj@nwu.edu.cn

1 Shaanxi Key Laboratory of Exploration and Comprehensive Utilization of Mineral Resources, Xi'an 710054, China

2 State Key Laboratory of Continental Dynamics, Northwest University, Xi'an 710069, China

3 Department of Geology, Northwest University, Xi'an 710069, China

4 Bureau of Geophysical Prospecting, CNPC, Zhuozhou 072751, China

5 CNPC Logging Changqing Business Division, Xi'an 710200, China

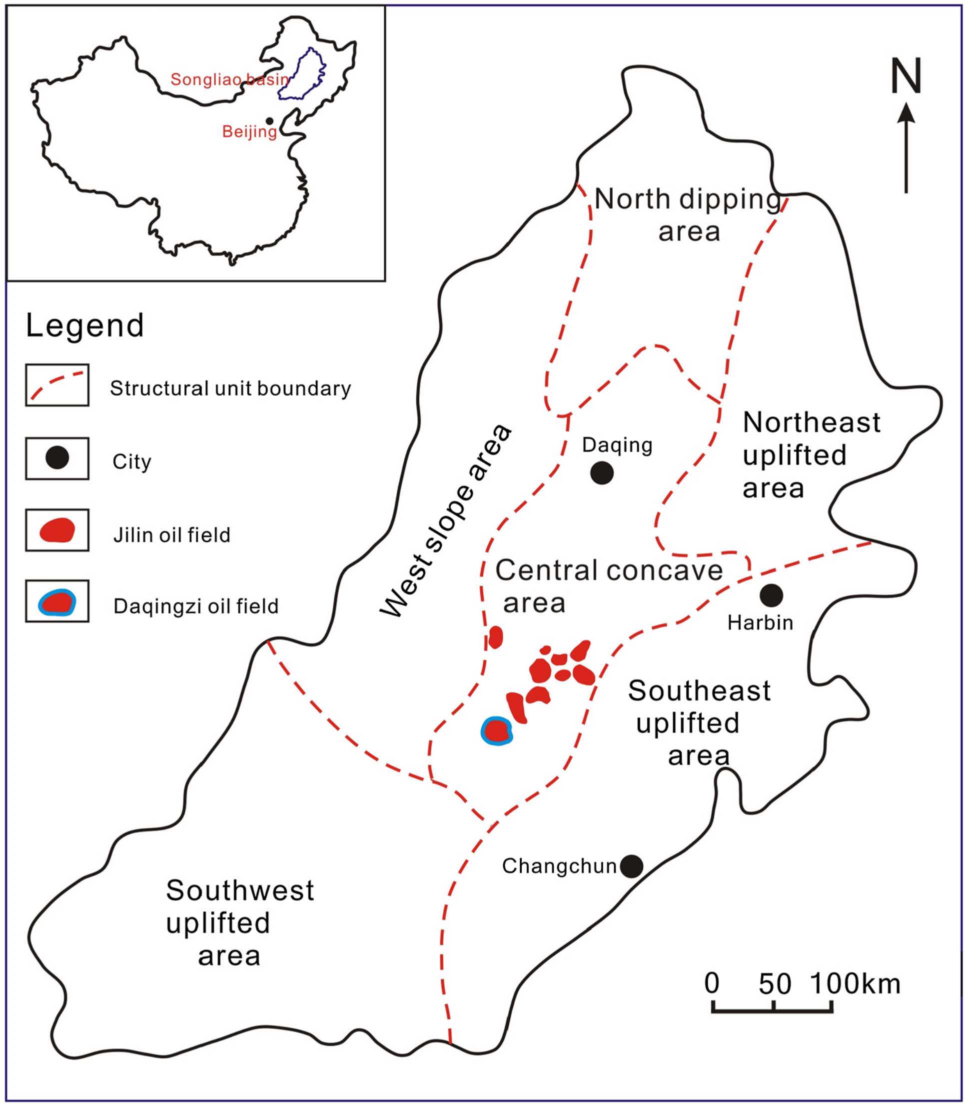

Fig. 1 Map of the location of the Daqingzijing oilfield (modified after Shu et al. 2003 with minor revisions)

sedimentary petrofacies of different types directly influence the effectiveness of the water injection. Specifically, water flooding of fine sandstone cross-beds is more effective than that of fine sandstone parallel beds. In distributary channels and subaqueous distributary channels, the development is ineffective, but the potential for remaining oil is the largest (Han 2007; Feng et al. 2012; Lin et al. 2013). Therefore, sedimentary petrofacies are of great importance for revealing the deposition mechanisms and distribution of a sand body of different geneses, reservoir heterogeneity and prediction, and the potential of remaining oil and for improving the ultimate recovery of the reservoir.

An integrated application of core, well logging, geology and other data must be based on comprehensive analysis of core observation and facies marks. This study is focused on the petrological characteristics, sedimentary petrofacies types, logging facies models and in-plane facies characteristics of the X–XII sand group of the K_2qn^3 Formation in the Daqingzijing area of the Songliao Basin, China. This study provides a geological basis for the description of a single sand body and its remaining oil trapping potential.

Geologic setting

The Songliao Basin is a large Meso–Cenozoic terrestrial petroliferous sedimentary basin located in Northeast China (Fig. 1) and covers a total area of 26 $\times$ 10^4 km^2. The basin has a diamond-shaped appearance, with its major axis expanding in the NNE direction. There are six sub-tectonic units in the basin, including the central concave area, southwest uplifted area, southeast uplifted area, northeast uplifted area, west slope area and north dipping area (Shu et al. 2003). The Daqingzijing oilfield is located in the southern part of the central concave area (Fig. 1). Its general structure is an asymmetric syncline, with its axis

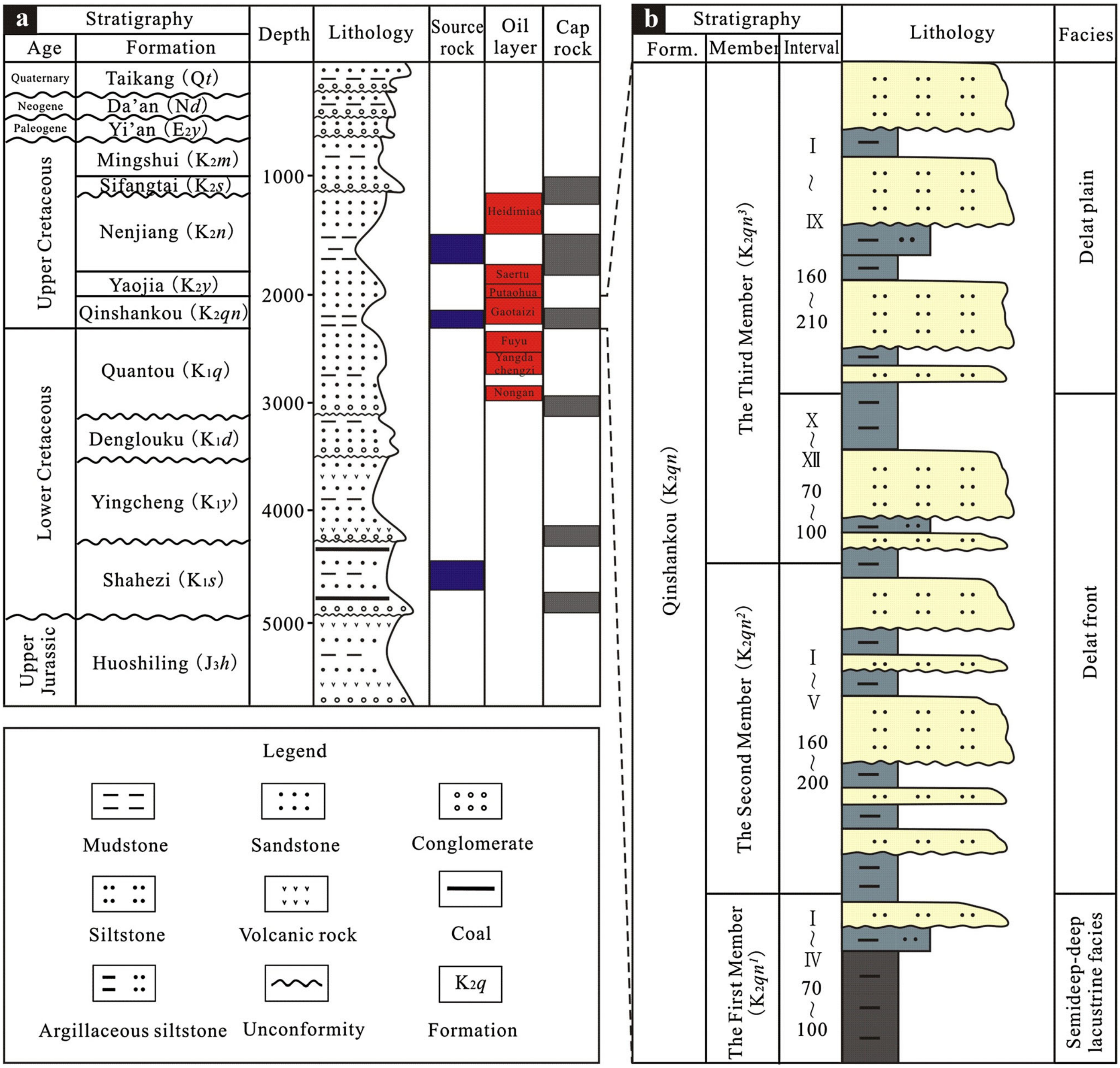

Fig. 2 Comprehensive stratigraphic column in the Daqingzijing area. **a** Stratigraphic distribution map of the Songliao Basin, **b** formation characteristics of the Qingshankou Formation in the Daqingzijing area, Songliao Basin

expanding in the NNE direction, displaying a gentle slope in the east and a steep slope in the west. The exploration area of Daqingzijing covers 1500 km^2, and the discovered reserves hold 100 million tons of crude oil. Its main target bed is the Cretaceous Qingshankou Formation. The oil layer is buried at a depth of approximately 1600–2500 m, and the sandstone reservoirs are characterized by low porosity, low permeability and low resistivity (Wei et al. 2007).

There are 4 sets of oil-bearing series in the Daqingzijing oilfield, which in ascending order are the Fuyu, Gaotaizi, Putaohua and Heidimiao oil reservoirs. The Gaotaizi oil layer of Qingshankou (K_2qn) is the main oil reservoir (Fig. 2a; Li et al. 2004). The Qingshankou includes Qing First Member (K_2qn^1), Qing Second Member (K_2qn^2) and Qing Third Member (K_2qn^3). The lithology of the Qing First Member mainly consists of gray-black and dark-gray shale, gray mudstone, sandstone and siltstone, developed with semi-deep lacustrine facies and deep lacustrine facies. It includes 4 sand groups, and its thickness ranges from 70 to 100 m. The lithology of Qing Second Member is mainly gray mudstone, argillaceous siltstone and siltstone, developed with delta front facies (Liu et al. 2014). It includes 5 sand groups, and its

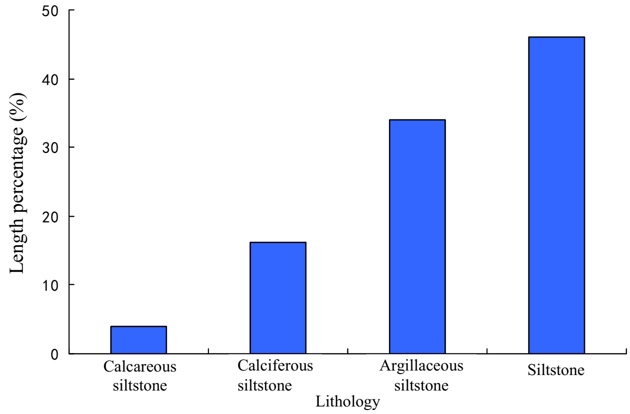

Fig. 3 Lithologic distribution histogram of the X–XII sand groups of the K_2qn^3 Formation in the Daqingzijing oilfield

thickness ranges from 160 to 200 m. The Qing Third Member is mainly composed of gray mudstone, aubergine mudstone, argillaceous siltstone and siltstone, developed with delta front and delta plain facies. It includes 12 sand groups, and its thickness ranges from 230 to 310 m (Fig. 2b; Wang et al. 2009; Liu et al. 2014).

Petrological characteristics

Lithology types

According to the statistical analysis of logging data acquired from Hei60, Hei120, Qian157-19-9 and Qian156 in the study area, the lithologies of the X–XII sand groups are mainly fine-grained sediments such as mudstone, argillaceous siltstone, calciferous siltstone, calcareous siltstone and siltstone (Fig. 3). The statistics show that of the rocks in the well core intervals, almost 46% are siltstone, approximately 34% are argillaceous siltstone, 16% are calciferous siltstone, and 4% are calcareous siltstone. Therefore, the main lithology of the study area is siltstone (Fig. 1).

Rock composition

According to a microscopic analysis using data acquired from Hei60, Hei120 and Qian157-19-9, rock particles in the study area mainly consist of quartz, feldspar and rock fragment (Fig. 4). Quartz contributes, on average, 38.5% of the rock petrofacies, with a range of 31.3–55.4%. The feldspar contributes a higher average content of 41.6%, with a range of 32–55%. The average content of rock fragment is 46.9%, with a range of 31.8–57%, and the rock fragment mainly originates from igneous rock. The cements are mainly clayey, and parts of them are calcareous.

Sedimentary petrofacies

The observation and description of 4 cored wells in the study area, combined with core analysis and laboratory data on size distribution, sedimentary structure and fossils of facies markers, resulted in the recognition of four different types of petrofacies in the study area.

Fig. 4 Rock composition of the X–XII sand groups of the K_2qn^3 Formation in the Daqingzijing oilfield

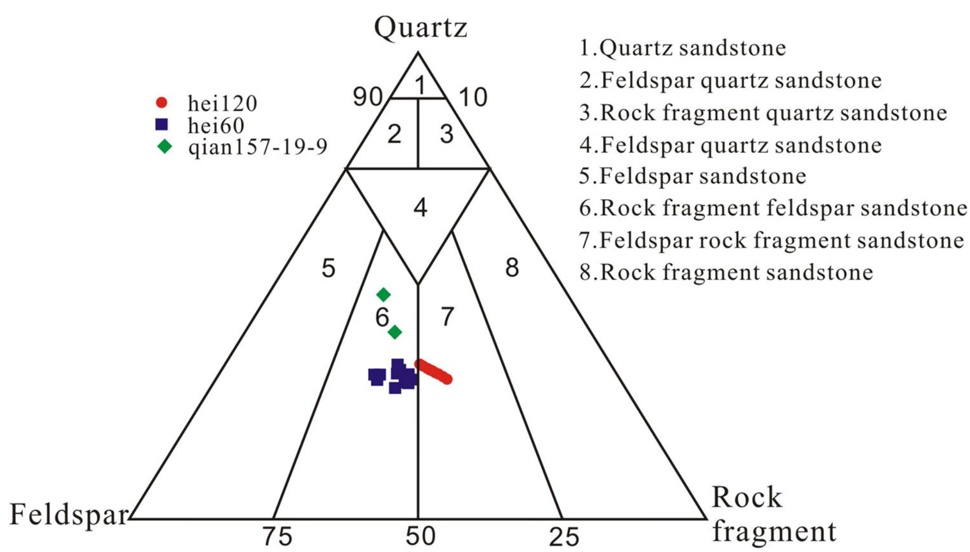

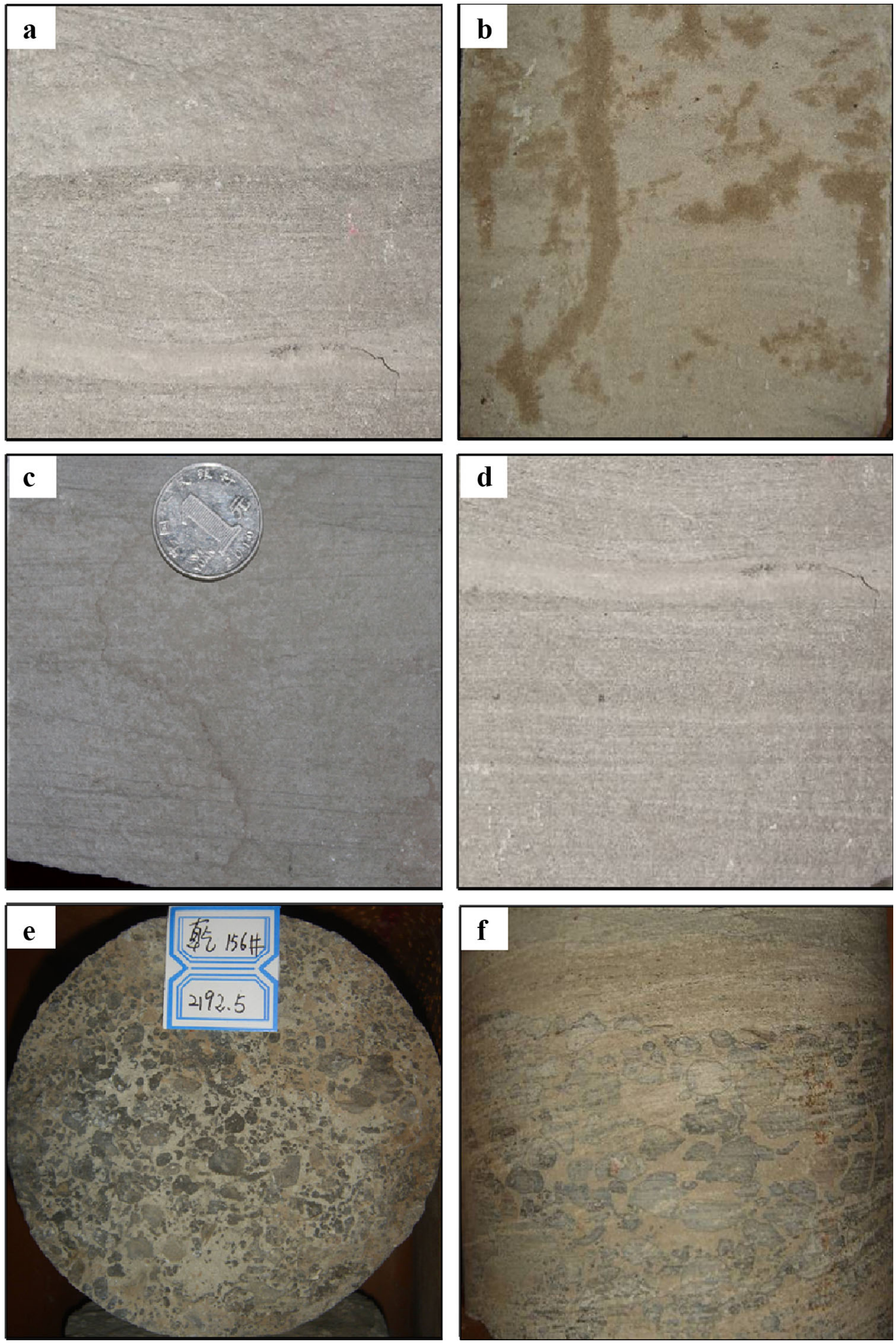

Fig. 5 Bedding structure of the X–XII sand groups of the K_2qn^3 Formation in the Daqingzijing oilfield. **a** Small cross-bedding in the Hei60 well core data, at a depth of 2185.3 m, **b** small cross-bedding in the Qian156 well core data, at a depth of 2207.8 m, **c** parallel bedding in the Hei60 well core data, at a depth of 2187 m, **d** parallel bedding in the Hei60 well core data, at a depth of 2185.8 m, **e** retention deposition in the Qian156 well core data, at a depth of 2192.5 m, **f** retention deposition in the Qian156 well core data, at a depth of 2191.4 m

Petrofacies type 1

Description

In the first petrofacies type of the study area, there are cross-beddings of small size, whose thickness ranges from a few cm to 10 cm. Large amounts of plant charcoal lamination, mud and mud gravel are observed in these small cross-beddings, making the lamina obscure. The laminated structure of the small cross-beddings can be seen by the enrichment of charcoal in local intervals (Fig. 5a, b).

There are also parallel beddings in the first petrofacies type of the study area, whose single-layer thickness ranges from 0.1 to 1.0 cm. Low-angle tilt can be seen in some laminations, often associated with small cross-beddings.

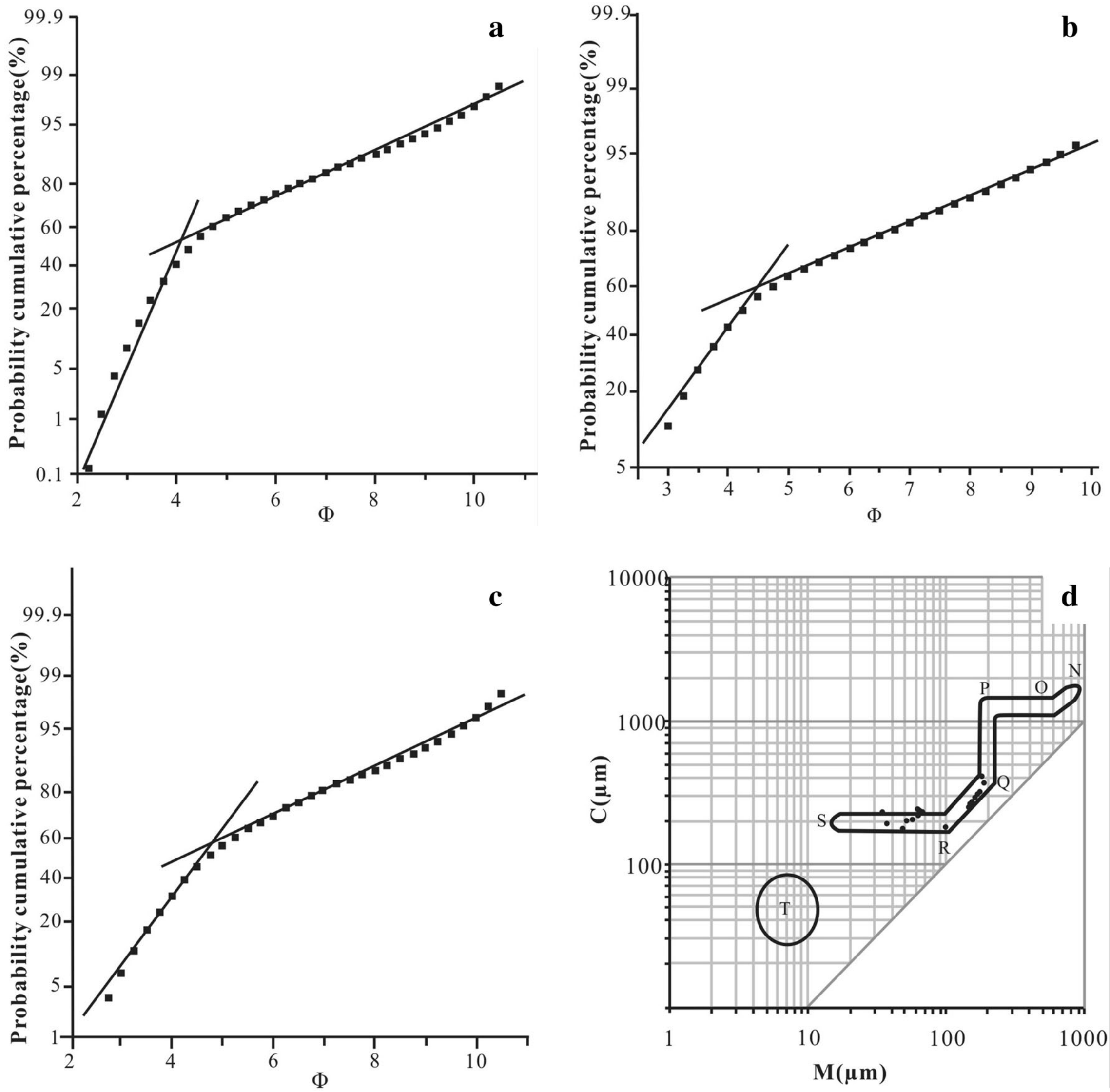

Fig. 6 Size analysis diagrams of the X–XII sand groups of the K_2qn^3 Formation in the Daqingzijing oilfield. **a** Particle size analysis of the Hei120 well core data, at a depth of 2238.7 m, **b** particle size analysis of the Hei120 well core data, at a depth of 2240.05 m, **c** particle size analysis of the Hei120 well core data at a depth of 2247.05 m, **d** C-M chart of the Hei120 well core data

Many parallel beddings are enriched with charcoal and lamina, which are usually shown by charcoal (Fig. 5c, d).

Erosion surface is the most common erosional structure of the X–XII sand groups of the K_2qn^3 Formation in the study area. Mud gravel is found above the erosion surface, and its thickness ranges from more than ten centimeters to tens of centimeters (Fig. 5e, f).

According to particle size analysis, using well core data acquired from Hei120, the particle size probability curve is mainly composed of two parts: a suspended part and a jump part. The jump content is 50–60%, and the size is mainly between 2 and 4.5 phi; the suspended content is 40–50%, and the size is greater than 4.5 phi (Fig. 6a–c). Based on the analysis of the particle size data, a C-M diagram was created, using well core data acquired from Hei120. The C-M diagram of the microphase mainly consists of QR and RS segments (Fig. 6d). QR and RS represent graded suspension deposition and uniform suspension deposition, respectively. Particle size analysis showed characteristics of a traction flow channel.

Interpretation: subaqueous distributary channel

The lithology of the first kind of petrofacies is mainly medium- to thick-bedded siltstone or argillaceous siltstone, which includes small cross-bedding and parallel bedding

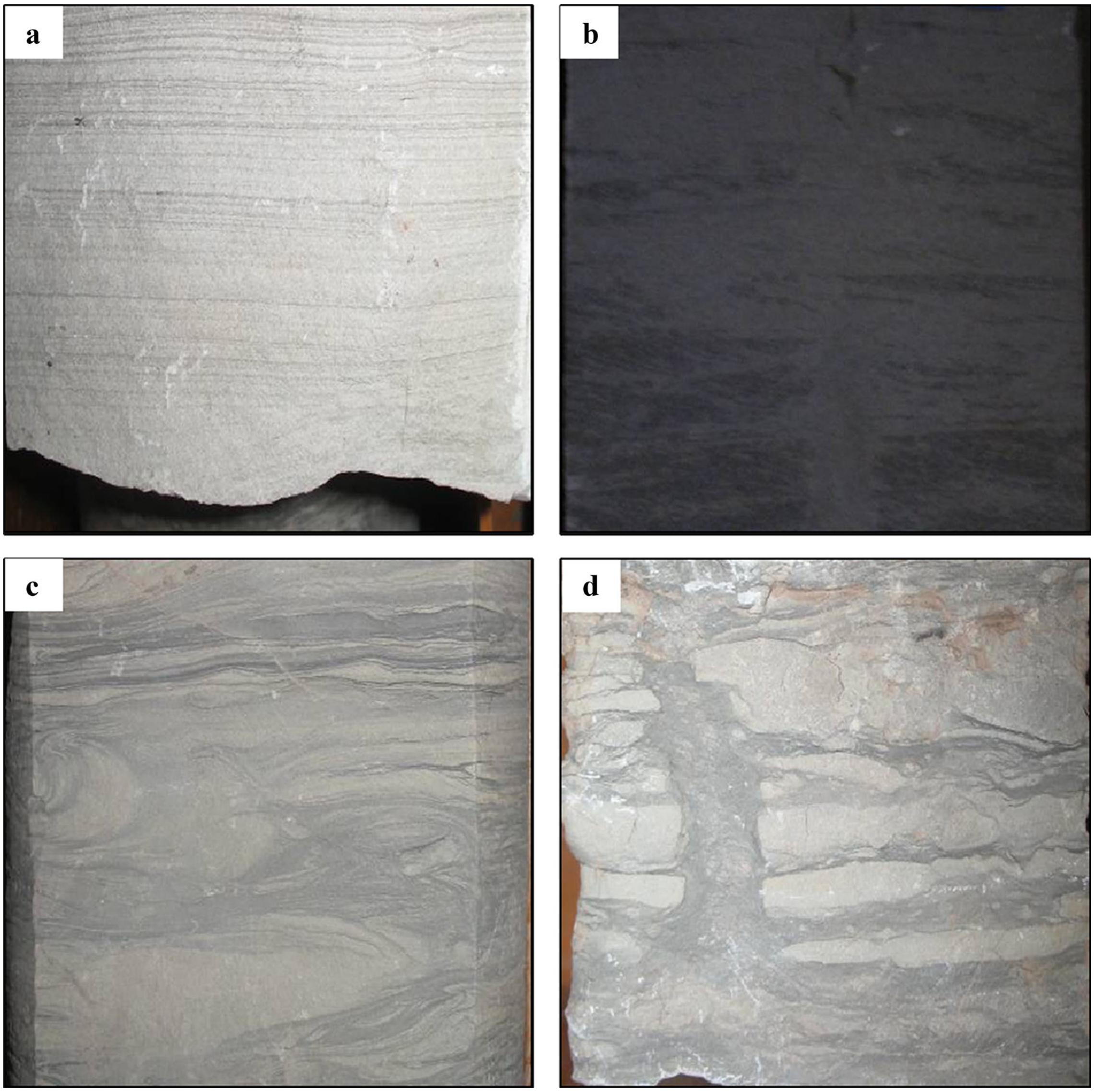

Fig. 7 Bedding structure of the X–XII sand groups of the K_2qn^3 Formation in the Daqingzijing oilfield. **a** parallel bedding in the Hei60 well core data, at a depth of 2188 m, **b** small cross-bedding in the Hei120 well core data, at a depth of 2249.55 m, **c** convoluted bedding in the Hei60 well core data, at a depth of 2189.3 m, **d** biological perturbation in the Hei60 well core data, at a depth of 2182.4 m

with thin lamina, reflecting weak hydrodynamic conditions. Erosion surface and lag deposits are observed, indicating it is in a channel system. The analysis of the grain size probability curve and C-M diagram shows that it is mainly composed of fine particles and two segment types. Traction flow is the main driving force for the material handling in this area. The vertical sequence is dominated by a positive rhythm, but a compound rhythm can also be seen. The logging curve is mainly characterized by a box- and bell-shaped appearance (Figs. 10a, 11). Therefore, the integrated interpretation shows that the first type of petrofacies is subaqueous distributary channel.

Petrofacies type 2

Description

The second type of petrofacies in the study area is characterized by thin-bedded sediments, containing parallel bedding (Fig. 7a) and small-scale cross-bedding (Fig. 7b). Its general thickness ranges from more than ten centimeters to tens of centimeters. The grain layer contains a layer of wood charcoal, which makes the lamina become less obvious; the lamina structure of the local layer is revealed by the enrichment of the carbon rock fragment.

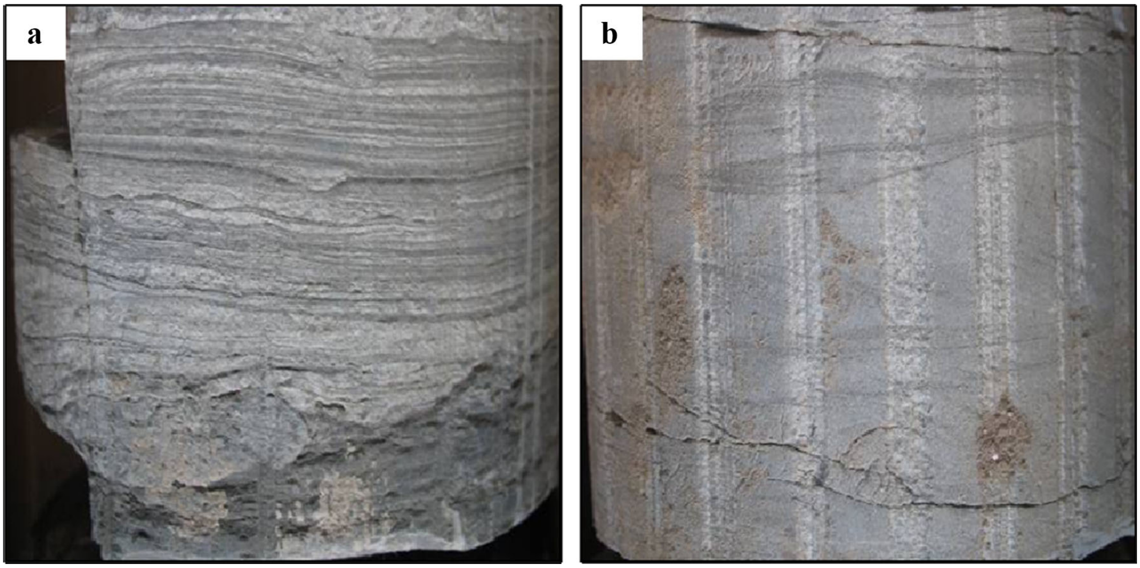

Fig. 8 Bedding structure of the X–XII sand groups of the K_2qn^3 Formation in the Daqingzijing oilfield. **a** Parallel bedding in the Qian157-19-9 well core data, at a depth of 2187.4 m, **b** ripple bedding in the Qian157-19-9 well core data, at a depth of 2210.4 m

Fig. 9 Mudstone of the X–XII sand groups of the K_2qn^3 Formation in the Daqingzijing oilfield. **a** Gray-black mudstone in the Qian157-19-9 well core data, **b** black mudstone in the Hei120 well core data

Deformed structures resulted from different degrees of local physical factors, between the deposition of the sediment and the consolidation of the rock. They are usually confined between the upper and lower layers. This convolution structure is very common and often present in siltstone and mudstone (Fig. 7c, d), indicating semi-consolidated sediments in a delta front sub-environment.

Interpretation: mouth bar

The lithology of the second petrofacies type is mainly siltstone and argillaceous siltstone, which includes small cross-bedding and thin lamina parallel bedding, suggesting weak hydrodynamic conditions. The electrical curve is funnel shaped, indicating coarsening-upward succession (Figs. 10b, 11). Therefore, the integrated interpretation shows that this second type is the mouth bar petrofacies.

Petrofacies type 3

Description

The third type of petrofacies in the study area is characterized by parallel bedding and ripple lamination. The

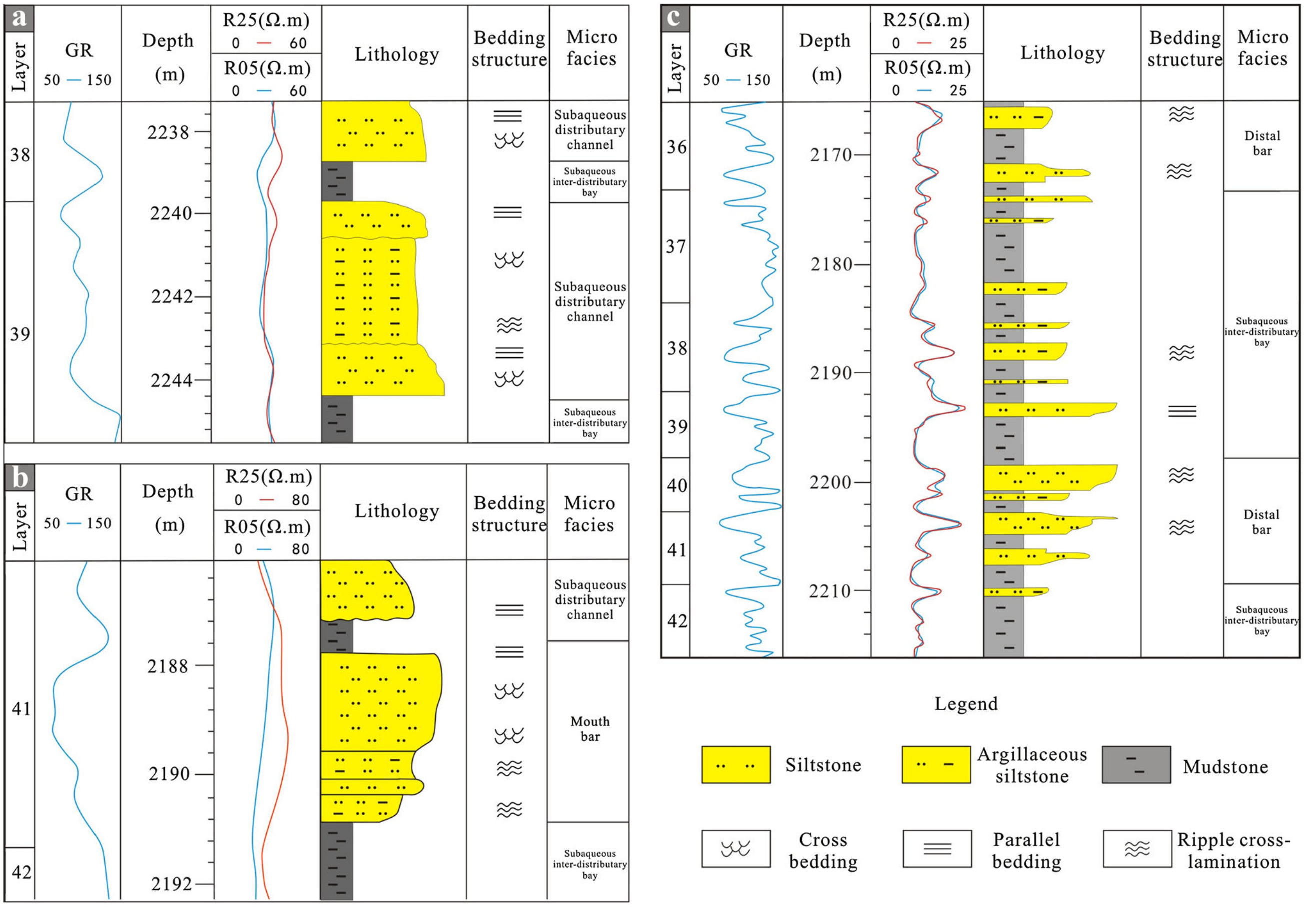

Fig. 10 Sedimentary petrofacies types of the K_2qn^3 Formation in the Daqingzijing oilfield. **a** Subaqueous distributary channel of the Hei120 well core data, **b** mouth bar of the Hei60 well core data, **c** distal bar and subaqueous interdistributary bay of the Qian157-19-9 well core data

parallel bedding is on a smaller scale, with the total laminae thickness ranging from a few centimeters to ten centimeters (Fig. 8a). Ripple lamination is often situated between the two sets of parallel beddings, which are smaller scale, with their overall thickness ranging from a few centimeters to ten centimeters. The local intervals of the lamina are fuzzy (Fig. 8b). Sand and mud interbed features are obvious, and part of the lamina shows dark mudstone.

Interpretation: distal bar

The lithology of the third petrofacies type is argillaceous siltstone and silty mudstone, which includes a thinner layer of parallel bedding and small ripple lamination, indicating overall weaker hydrodynamic conditions. Interaction between sand and mud occurs from bottom to top, the clay content increases without any rhythm, and the shape of well logging curve is zigzag (Figs. 10c, 11). Therefore, the integrated interpretation shows that the third type is the distal bar petrofacies.

Petrofacies type 4

Description

The fourth petrofacies type in the study area is mainly mudstone, mostly colored light gray, gray, gray-green, gray-black and several types of black mudstone (Fig. 9). The petrofacies mudstone thickness is relatively high, and horizontal laminations can be found.

Interpretation: subaqueous interdistributary bay

The lithology of the fourth petrofacies is mainly silty mudstone; its color is gray, gray-green and gray-black, generally reflecting weak oxidation and weak reduction of the shallow to semi-deep aquatic sedimentary environment. It contains horizontal and wavy bedding, formed in extremely weak hydrodynamic conditions by the suspension of fine-grained sediments and continuous sedimentation, an important characteristic of hydrostatic or low-energy environments. Finally, the logging curve is a flatter curve

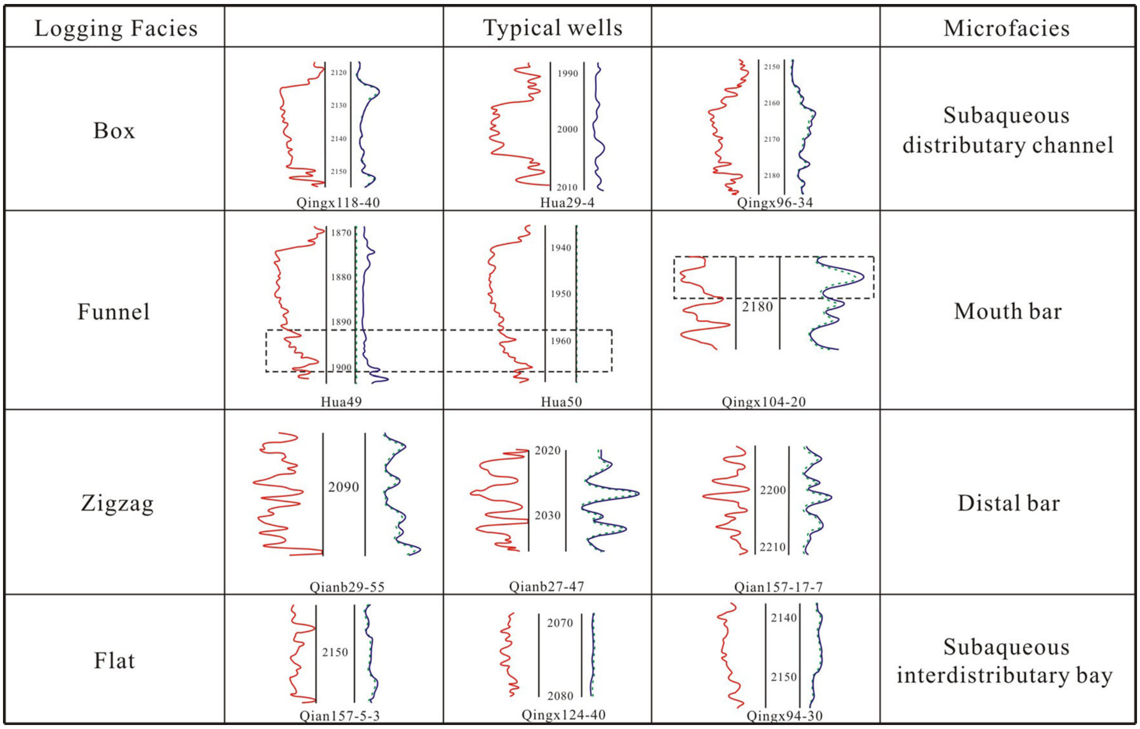

Fig. 11 Logging facies types of the K_2qn^3 Formation in the Daqingzijing oilfield

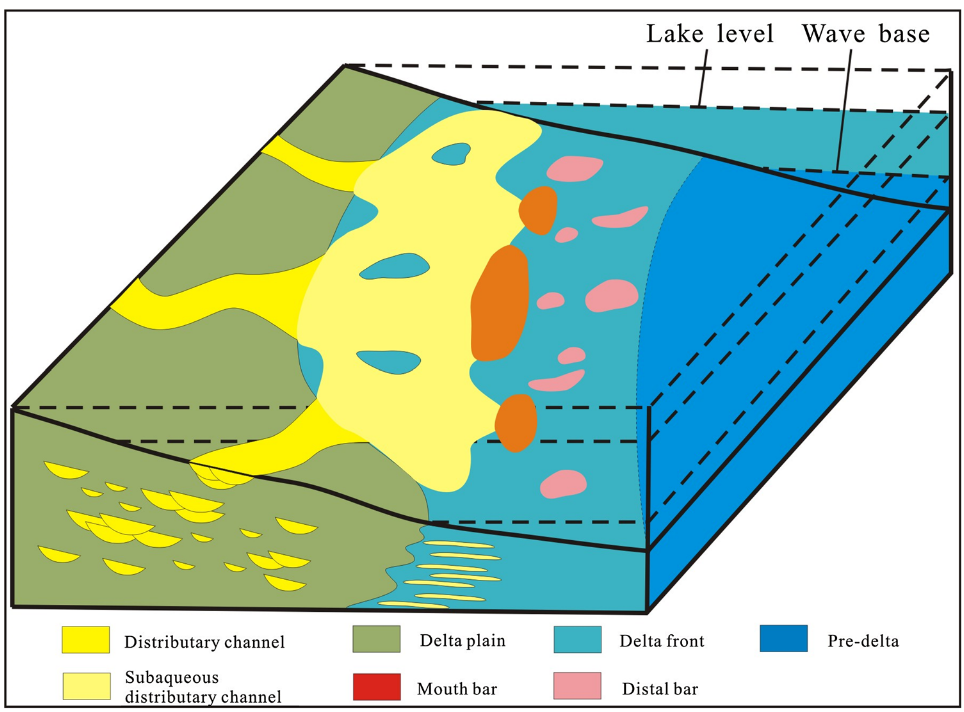

Fig. 12 Sedimentary facies model of the X–XII sand group in the K_2qn^3 Formation in the Daqingzijing oilfield

(Figs. 10c, 11). Therefore, the integrated interpretation of the fourth petrofacies type is the subaqueous interdistributary bay.

To summarize the sedimentary characteristics of the four different kinds of petrofacies in the study area, the overall color of the mudstone is mainly gray to black, which reflects conditions of weak oxidation and reduction. The cross-beddings and parallel beddings are smaller scale, reflecting weak hydrodynamic conditions. The distal bar is developing, and the phenomenon of biological disturbance is obvious, which reflects characteristics of shallow-water deposition. Therefore, the sedimentary environment of the study area is interpreted as a shallow-water delta front. Based on the analysis of the petrofacies types from the well core data, the well logging facies models of the different types were established based on rock electric calibration (Fig. 11). The sedimentary petrofacies types of non-cored wells can be explained according to the logging curves of different types.

In-plane facies analysis and facies model

In-plane facies analysis

Based on the recognition of the petrofacies types in the cored wells, the petrofacies identification of the non-cored wells in the study area was carried out by using the well logging facies models of different petrofacies. According to the thickness of the sand body of each layer, the in-plane facies of each layer are drawn with the type of sedimentary petrofacies of different wells.

Take the XI sand group as an example to describe the different sedimentary petrofacies characteristics of Layer 36. Layer 36 contains mainly delta front deposition, the source direction is southwest and west, and multistage subaqueous distributary channel sand bodies are stacked to form a composite sand body with large area and sheet distribution. Mouth bar petrofacies are relatively small, mainly developed in subaqueous distributary channels. Different-scale distal bar petrofacies are suggested in the northeast of the study area.

Facies model

Based on previous studies (Wei et al. 2007), combined with regional sedimentary background knowledge, we propose a shallow-water delta model in study area of the K_2qn^3 Formation in the Daqingzijing oilfield (Fig. 12). The depositional model includes subaqueous distributary channel, subaqueous interdistributary bay, mouth bar, distal bar and pre-delta mudstone.

Conclusion

1. The petrofacies of the X–XII sand group in the study area mainly include parallel bedding siltstone, cross-bedding siltstone, ripple lamination siltstone and horizontal lamination mudstone. Cross-bedding siltstone thickness ranges from a few cm to 10 cm, and the laminated structure of the cross-bedding can be seen by the enrichment of charcoal in local intervals. Parallel bedding siltstone thickness ranges from 0.1 to 1.0 cm, often associated with cross-bedding. Ripple lamination siltstone is smaller scale, and its overall thickness ranges from a few centimeters to ten centimeters. The colors of horizontal lamination mudstone mainly include light gray, gray, gray-green and gray-black, and its thickness is relatively high.
2. The core observation, description and facies analysis showed that the studied interval was deposited on a shallow-water delta front depositional environment, which included four sub-environments: subaqueous distributary channel, subaqueous interdistributary bay, mouth bar and distal bar. The well logging facies models are established based on the different types of petrofacies, and the recognition of the petrofacies types of non-cored well core data was completed.

Acknowledgements This work was financially supported by Opening Foundation of Shaanxi Key Laboratory of Exploration and Comprehensive Utilization of Mineral Resources; Scientific Research Project from Shaanxi Province Department of Education (14JK1754). The authors would like to thank the editor and two anonymous reviewers for their critical reviews, which led to much improvement of this paper.

References

Cao YC, Han M, Wang YZ (2010) Sedimentary characteristics and models of shallow-water delta deposits in the second member of the Shahejie Formation in the Chezhen Sag, the Jiyang Depression. Oil Gas Geol 31(5):576–601

Er C, Niu JY, Gu JY, Li GP, Li XG, Kang WJ, Liu B, Yang JY (2013) Characteristics of main sedimentary facies distribution and depositional controls of E_2s^3 in shuangtaizi structure belt, Liaohe depression. Acta Sedimentol Sin 31(6):1106–1113

Feng CJ, Bao ZD, Chen BC, Wei ZS, Wang Y (2012) Application of the single factor analysis and multi-factor coupling method to the remaining oil prediction in Fuyu oilfield. Acta Pet Sin 33(3):445–471

Feng CJ, Shan QT, Shi WC, Zhu SW (2013) Reservoirs heterogeneity and its control on remaining oil distribution of K_1q^4, Fuyu oilfield. J China Univ Pet 37(1):1–7

Han DK (2007) Precisely predicting abundant remaining oil and improving the secondary recovery of mature oilfields. Acta Pet Sin 28(2):73–78

Li JZ, Yang T, Wang LW, Jiang T (2004) The fault structure and its controlling role to hydrocarbon accumulation in Daqingzijing area, Southern Songliao Basin. Pet Explor Dev 31(1):18–20

Li Y, Zhu XM, Song YQ, Liu F, Li C (2013) Sedimentary characteristics and evolution of shallow water delta of the lower cretaceous Fuyu reservoir in the Yushulin oilfield, Songliao Basin. Geol J China Univ 19(1):23–31

Lin CY, Dong CM, Ren LH, Zhang XG, Xin QL, Liu ZR (2013) Development of reservoir characterization and its stimulation. J China Univ Pet 37(5):22–27

Liu ZJ, Sun PC, Liu R, Meng QT, Bai YY, Xu YB (2014) Research on geological conditions of shale coexistent energy mineralization (accumulation): take the Qingshankou Formation in Upper Cretaceous, Songliao Basin for example. Acta Sedimentol Sin 32(3):593–600

Shu L, Mu Y, Wang C (2003) The oil–gas-bearing strata and the structural features in the Songliao Basin, China. J Stratigr 27(4):340–347

Wang JG, Wang TQ, Wei PS, Shi LT, Han XQ, Liu CY, Shi YS (2009) Identification of unconformity plane at the bottom (K_2qn^3) of Qingsan Member in the Songliao Basin and its implication for petroleum geology. Acta Geol Sin 83(1):79–88

Wei ZS, Song XM, Tang ZX, Chu X, Yang G (2007) Sedimentary facies and lithologic oil pools of the Upper Cretaceous Qingshankou Formation in Daqingzijing area, Changling Sag, Southern Songliao Basin. Pet Explor Dev 43(1):28–33

Zeng HL, Zhu XM, Zhu RK, Zhang QS (2013) Seismic prediction of sandstone diagenetic facies: applied to Cretaceous Qingshankou Formation in Qijia Depression, Songliao Basin. Pet Explor Dev 40(3):266–274

Zhang DW, Chen FJ, Cheng G (2006) The microscopic features of pore structure in Gaotaizi oil layer of Daqingzijing area. Oil Geol 27(5):668–674

Zhang QG, Bao ZD, Na WH, Zhou XM, Sun JW (2007) Sedimentary facies of the Member 4 of Quantou Formation of lower Cretaceous in southern central depression of Songliao Basin. J Palaeogeogr 19(3):267–276

Zhang Z, Bao ZD, Tong HM, Wang Y (2009) Sedimentary facies and facies model of the 3rd member of Shahejie formation in the Western Liaohe Sag Fault Basin. Geol J China Univ 15(3):387–397

Zhang CM, Yin TJ, Zhu YJ, Ke LM (2010) Shallow water deltas and models. Acta Sedimentol Sin 28(5):933–944

Zhang S, Cui KN, Zhang CC, Jin MY (2011) Controlling factors and distribution patterns of lithologic pools in the fluvial facies of the 3rd and 4th members of the Quantou Formation in the Songliao Basin. Oil Geol 32(3):411–419

Zhu XM, Liu Y, Fang Q, Li Y, Liu YY, Wang R, Song J, Liu SQ, Cao HT, Liu XN (2012) Formation and sedimentary model of shallow delta in large-scale lake, example from Cretaceous Quantou Formation in Sanzhao Sag, Songliao Basin. Earth Sci Frontiers 19(1):89–99

Zou CN, Xue SH, Zhao WZ, Li M, Wang YC, Liang CX, Zhao ZK, Zhao ZY (2004) Depositional sequences and forming conditions of the Cretaceous stratigraphic-lithologic reservoirs in the Quantou-Nengjiang Formations, South Songliao Basin. Pet Explor Dev 31(2):16–19

Publisher's Note